Array Design for Increased Spatial Aliasing Frequency in Wave Field Synthesis Based on a Geometric Model*

Fiete Winter, Frank Schultz, Sascha Spors

Institute of Communications Engineering, University of Rostock, R.-Wagner-Str. 31, 18119 Rostock, Germany,
Email: {fiete.winter; frank.schultz; sascha.spors}@uni-rostock.de

1 Introduction

Wave Field Synthesis (WFS) aims at a physically accurate synthesis of a desired sound field inside a target region. Typically, the region is surrounded by a finite number of discrete loudspeakers. For practical loudspeaker setups, this spatial sampling causes spatial aliasing artefacts and does not allow for an accurate synthesis over the entire audible frequency range. Recently, the authors proposed a geometric model to predict the so-called aliasing frequency up to which the spatial aliasing is negligible for a specific listening position or area [1]. Besides its dependency on the desired sound field, this frequency is influenced by the spacing between individual loudspeakers. The present work discusses the effects of non-uniform spacing on the aliasing frequency, see Sec. 4.1. Optimal discretisation patterns for a given array geometry and desired sound field are derived in Sec. 4.2. The patterns are compared to a uniform sampling scheme via numerical simulations of the synthesised sound fields in Sec. 5.

2 Preliminaries

A sound pressure field $p(\mathbf{x}, t)$ is a scalar function depending on position $\mathbf{x}$ and time t. Its temporal Fourier transform $P(\mathbf{x}, \omega) = A_P(\mathbf{x}, \omega)\, \mathrm{e}^{+\mathrm{j}\phi_P(\mathbf{x},\omega)}$ is expressed by its real-valued amplitude $A_P(\mathbf{x}, \omega)$ and phase $\phi_P(\mathbf{x}, \omega)$, here. The radial frequency $\omega = 2\pi f$ is defined by the temporal frequency f. For an arbitrary sound field fulfilling the linear wave equation, the local wavenumber vector is defined for $\mathrm{e}^{+\mathrm{j}\omega t}$ convention as [2, Eq. (15)].

$$\mathbf{k}_P(\mathbf{x}, \omega) := -\operatorname{grad} \phi_P(\mathbf{x}, \omega) \approx \frac{\omega}{\mathrm{c}}\, \hat{\mathbf{k}}_P(\mathbf{x}, \omega)\,. \qquad (1)$$

The speed of sound is denoted by c and is fixed to $343\,\mathrm{m/s}$ for all simulations within this paper. The normalised vector $\hat{\mathbf{k}}_P(\mathbf{x}, \omega)$ describes the local propagation direction of $P(\mathbf{x}, \omega)$ at a given coordinate $\mathbf{x}$. For elementary sound fields such as point and line sources, or plane waves, $\mathbf{k}_P(\mathbf{x}, \omega)$ fulfils the local dispersion relation, i.e. its length is fixed to ω/c. For arbitrary sound fields, this statement is true for asymptotically high frequencies, see [3, Sec. 5.14].

3 Wave Field Synthesis

WFS is a method for Sound Field Synthesis (SFS). Its fundamental task is to synthesise the virtual sound field $S(\mathbf{x}, \omega)$ within a defined region Ω, see Fig. 1. In $2\frac{1}{2}$-dimensional (2.5D) scenarios [4, Sec. 2.3], correct synthesis is pursued in the horizontal plane ($z = 0$) using a Secondary Source Distribution (SSD) located in the same plane ($z_0 = 0$). Thus, Ω is a 2D area. Within the described scenario, it is assumed that the virtual sound field does only propagate in horizontal directions, i.e. the z-component of its local wavenumber vector $\mathbf{k}_S(\mathbf{x}, \omega)$ is zero for $z = 0$. The boundary $\partial\Omega$ is described as a curve $\mathbf{x}_{0,u}(u)$ depending on the parameter $u \in [u_{\min}, u_{\max}]$. The component-wise derivative of $\mathbf{x}_0$ w.r.t. u is denoted as $\mathbf{x}'_{0,u}(u)$. It is oriented along the unit tangent vector $\mathbf{t}_0$. The inward pointing boundary normal vector $\mathbf{n}_{0,u}(u)$ is perpendicular to $\mathbf{x}'_{0,u}(u)$ and $\mathbf{t}_{0,u}(u)$. A distribution of loudspeakers is positioned along the boundary $\partial\Omega$ as secondary sources (see the loudspeaker symbols in Fig. 1). Each secondary source is oriented along $\mathbf{n}_{0,u}(u)$. The sound field emitted by an individual secondary source is commonly modelled by a point source. It is given by the 3D free-field Green's function $G(\mathbf{x}-\mathbf{x}_0, \omega)$ [5, Eq. (8.41)]. The secondary source at $\mathbf{x}_0$ is driven by its respective driving function $D(\mathbf{x}_0, \omega)$ and the resulting wave field superposition of all secondary sources constitutes the synthesised sound field

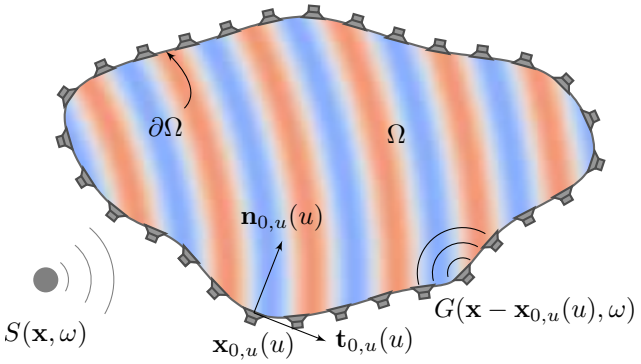

Figure 1: Geometry for Wave Field Synthesis

$$P(\mathbf{x}, \omega) = \int_{u_{\min}}^{u_{\max}} D(\mathbf{x}_{0,u}(u), \omega) \cdot G(\mathbf{x} - \mathbf{x}_{0,u}(u), \omega) |\mathbf{x}'_{0,u}(u)|\, \mathrm{d}u. \qquad (2)$$

The generic 2.5D WFS driving function and approximate solution of the integral is given by [1, Eq. (8b)]

$$D(\mathbf{x}_0, \omega) = a_S(\mathbf{x}_0) \sqrt{\mathrm{j}\frac{\omega}{\mathrm{c}}} \sqrt{8\pi d(\mathbf{x}_0)}\, \mathbf{n}_0^{\mathrm{T}} \hat{\mathbf{k}}_S(\mathbf{x}_0, \omega) S(\mathbf{x}_0, \omega)\,. \qquad (3)$$

The secondary source selection criterion $a_S(\mathbf{x}_0)$ [2, Eq. (46)] activates only the secondary sources that are oriented along the propagation direction of the virtual sound field. Within this paper, the the support

*This research was supported by grant SP 1295/9-1 of the German Research Foundation (DFG). The code to reproduce the simulations in the paper is available under GNU General Public License v3 at `https://doi.org/10.5281/zenodo.2594852`.

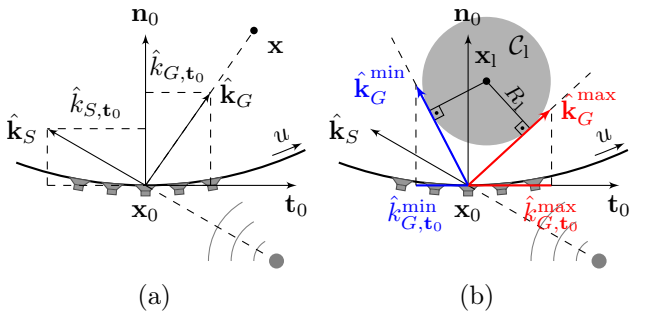

Figure 2: (a) shows the geometry for the spatial aliasing frequency at a single position $\mathbf{x}$ and a virtual point source (grey dot). (b) illustrates an analogous scenario for a circular listening area $\mathcal{C}_\mathrm{l}$.

$[u_\mathrm{min}, u_\mathrm{max}]$ already incorporates the selection. As one systemic artefact in 2.5D synthesis, an inevitable mismatch between the amplitude decay of the synthesised and the virtual sound field occurs. The function $d(\mathbf{x}_0)$ can be used to reference the synthesised sound field to a given contour/location on/at which its amplitude is correct. For more details, see [2].

4 Spatial Discretisation and Aliasing

The practical implementation of WFS implies the discretisation of the continuous SSD as the distance between adjacent loudspeakers cannot be chosen arbitrarily small. For a uniform sampling w.r.t. u the synthesised sound field is approximated by

$$P^\mathrm{S}(\mathbf{x},\omega) = \sum_{n=0}^{N_0-1} D(\mathbf{x}_{0,u}(u_\mathrm{min}+n\Delta_u),\omega) \cdot G(\mathbf{x}-\mathbf{x}_{0,u}(u_\mathrm{min}+n\Delta_u),\omega)|\mathbf{x}'_{0,u}(u_\mathrm{min}+n\Delta_u)|\Delta_u\,. \tag{4}$$

with the u-domain sampling distance $\Delta_u = {u_\mathrm{max}-u_\mathrm{min}}/{N_0-1}$ in the u-domain. The number of secondary sources is denoted by N_0. It should be noted, that there exist an infinite number of parametrisations describing the same boundary. For example, the two parametrisations $\mathbf{x}_{0,u}(u) = [u,0,0]^\mathrm{T}$ for $u \in [-1,1]$ and $\mathbf{x}_{0,v}(v) = [v^3,0,0]^\mathrm{T}$ for $v \in [-1,1]$ define the same finite linear SSD. However, an equidistant sampling w.r.t u and v lead to different spacing schemes. In the following, a connection between the parametrisation and the spatial aliasing is established. Further, an optimal parametrisation to avoid aliasing is derived.

4.1 Spatial Aliasing Frequency

In [1], a geometric model was introduced to predict the spatial aliasing frequency and to describe the aliasing properties for a given SFS scenario. The derived frequencies exhibit the mathematical structure given by

$$f^\mathrm{S} = \min_u f^\mathrm{S}_u(u) = \min_u \frac{\mathrm{c}}{\underbrace{|\mathbf{x}'_{0,u}(u)|\cdot\Delta_u}_{=\Delta_{\mathbf{x}_0,u}(u)}\cdot\gamma(\mathbf{x}_{0,u}(u))}\,, \tag{5}$$

where $f^\mathrm{S}_u(u)$ denotes the (local) aliasing frequency of a distinct secondary source position $\mathbf{x}_0(u)$. The minimum over all secondary sources yields the aliasing frequency f^S. $\Delta_{\mathbf{x}_0,u}(u)$ is the local sampling distance in Cartesian space. The scenario-dependent function is denoted as γ. For the aliasing frequency of a single listening position $\mathbf{x}$, it reads [1, Eqs. (35)]

$$\gamma(\mathbf{x}_0) = \left|\hat{k}_{S,\mathbf{t}_0}(\mathbf{x}_0) - \hat{k}_{G,\mathbf{t}_0}(\mathbf{x}-\mathbf{x}_0)\right|. \tag{6}$$

The explanatory geometry is shown in Fig. 2a: $\hat{k}_{S,\mathbf{t}_0}(\mathbf{x}_0)$ denotes the tangential component of the normalised wavenumber vector $\hat{\mathbf{k}}_S$ for the virtual sound field. It is equal to the cosine of the angle between the tangent $\mathbf{t}_0$ and the propagation direction of the virtual sound field at $\mathbf{x}_0$. $\hat{k}_{G,\mathbf{t}_0}(\mathbf{x}-\mathbf{x}_0)$ denotes the tangential component of the normalised wavenumber vector $\hat{\mathbf{k}}_G$ of the Green's function. It is equal to the cosine of the angle between $\mathbf{t}_0$ and $\mathbf{x}-\mathbf{x}_0$.

For a circular area $\mathcal{C}_\mathrm{l}$ with centre $\mathbf{x}_\mathrm{l}$ and radius R_l, see Fig. 2b, the term is given by [1, Eq. (38)]

$$\gamma(\mathbf{x}_0) = \max\left(\left|\hat{k}^\mathrm{max}_{G,\mathbf{t}_0}(\mathbf{x}_0) - \hat{k}_{S,\mathbf{t}_0}(\mathbf{x}_0)\right|; \left|\hat{k}^\mathrm{min}_{G,\mathbf{t}_0}(\mathbf{x}_0) - \hat{k}_{S,\mathbf{t}_0}(\mathbf{x}_0)\right|\right) \tag{7}$$

with $\hat{k}^\mathrm{min}_{G,\mathbf{t}_0}(\mathbf{x}_0)$ and $\hat{k}^\mathrm{max}_{G,\mathbf{t}_0}(\mathbf{x}_0)$ denoting the minimum and maximum values for the tangential component of the Green's function. They are given by [1, Eq. (61)]

$$\hat{k}^{\{\mathrm{min,max}\}}_{G,\mathbf{t}_0}(\mathbf{x}_0) = \begin{cases} \mp 1 & \text{if } \varrho > 1\,, \text{ else} \\ \mp 1 & \text{if } \hat{k}_{l,\mathbf{t}_0} \lessgtr \sqrt{1-\varrho^2}\,, \\ \hat{k}_{\mathrm{l},\mathbf{t}_0}\sqrt{1-\varrho^2} \mp \varrho\sqrt{1-\hat{k}^2_{\mathrm{l},\mathbf{t}_0}} & \text{otherwise,} \end{cases} \tag{8}$$

where the upper and lower option for $\mp$ and $\lessgtr$ applies for $\hat{k}^\mathrm{min}_{G,\mathbf{t}_0}(\mathbf{x}_0)$ and $\hat{k}^\mathrm{max}_{G,\mathbf{t}_0}(\mathbf{x}_0)$, respectively. ϱ defines the ratio ${R_\mathrm{l}}/{|\mathbf{x}-\mathbf{x}_\mathrm{l}|}$ and $\hat{k}_{\mathrm{l},\mathbf{t}_0} = \hat{k}_{G,\mathbf{t}_0}(\mathbf{x}_\mathrm{l}-\mathbf{x}_0)$. In order of appearance, the different cases cover scenarios, where the circle includes $\mathbf{x}_0$, intersects with the boundary $\partial\Omega$ without including $\mathbf{x}_0$, or is completely inside Ω. For $R_\mathrm{l} \to 0$, the circle degenerates to a single position. Thus, (7) coincides with (6). For the case $R_\mathrm{l} \to \infty$,

$$\gamma(\mathbf{x}_0) = |\hat{k}_{S,\mathbf{t}_0}(\mathbf{x}_0)| + 1 \tag{9}$$

holds, which corresponds to the aliasing frequency for arbitrary listening positions. If the virtual sound field is unknown or arbitrary, the extremal values ± 1 may be assumed for $\hat{k}_{S,\mathbf{t}_0}(\mathbf{x}_0)$. The resulting function reads [1, Eq. (39)]

$$\gamma(\mathbf{x}_0) = 1 + \max\left(\left|\hat{k}^\mathrm{max}_{G,\mathbf{t}_0}(\mathbf{x}_0)\right|; \left|\hat{k}^\mathrm{min}_{G,\mathbf{t}_0}(\mathbf{x}_0)\right|\right). \tag{10}$$

The common structure for the spatial aliasing frequency in (5) allows for a general discussion: it exhibits a dependency on $|\mathbf{x}'_{0,u}(u)|$ and $\gamma(\mathbf{x}_{0,u}(u))$. The function γ, however, depends only on the secondary source position $\mathbf{x}_0$. As long as two parametrisations $\mathbf{x}_{0,u}(u)$ and $\mathbf{x}_{0,v}(v)$ describe the same curve, γ is independent of the actual choice of parametrisation. However, extremal values of the first-order derivatives $|\mathbf{x}'_{0,u}(u)|$ and $|\mathbf{x}'_{0,v}(v)|$ are not invariant in that regard. The question arises, which parametrisation is optimal w.r.t. the resulting aliasing frequency.

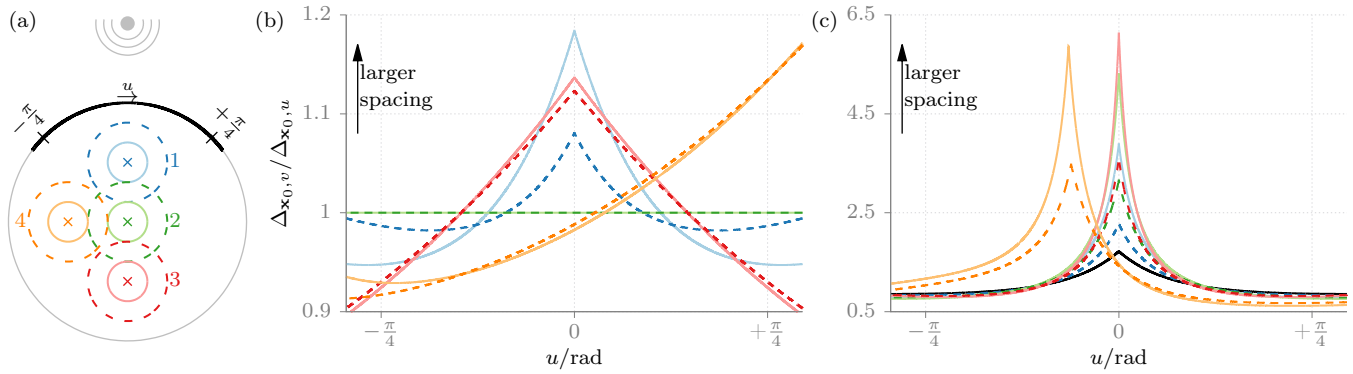

Figure 3: (a) depicts evaluation scenario. A virtual point source (grey dot) is supposed to be synthesised by the circular SSD whose active part is illustrated by the black line. The spacing is optimised for eight circular areas $\mathcal{C}_\mathrm{l}$ centred at $\mathbf{x}_\mathrm{l}$ (crosses) with the radii $R_\mathrm{l} = 0.25$ m (solid) and $R_\mathrm{l} = 0.5$ m (dashed). The remaining plots show the ratio between optimised SSD spacing $\Delta_{\mathbf{x}_0,v}$ and the equiangular spacing $\Delta_{\mathbf{x}_0,u}$ as a function of the parameter u. In (b), the spacing is optimised w.r.t. the aliasing frequency of $\mathcal{C}_\mathrm{l}$ for arbitrary sound fields (10). The colours and dash patterns correspond to the circles in (a). The analogous results for sound field specific aliasing frequency (7) are shown in (c). The black line corresponds to the optimisation w.r.t. (9).

4.2 Optimal Spacing

It is assumed, that a (suboptimal) parametrisation $\mathbf{x}_{0,u}(u)$ is given and allows to explicitly calculate the secondary source positions. On the other side, $\mathbf{x}_{0,v}(v)$ is the optimal, yet unknown parametrisation. Since $\mathbf{x}_{0,u}(u)$ and $\mathbf{x}_{0,v}(v)$ describe the same boundary, there is a pair of u and v describing the same secondary source position $\mathbf{x}_0$. Due to the bijective mapping between the two parameters, v may be expressed as a function of u, i.e. $v(u)$. The bijectivity requires $v(u)$ to be either strictly increasing or decreasing. Without loss of generality, it is assumed that $v'(u) > 0$ (for increasing $v(u)$) and both parameters share the same support, i.e. $u_\mathrm{max} = v(u_\mathrm{max})$, $u_\mathrm{min} = v(u_\mathrm{min})$, and $\Delta_u = \Delta_v$. Equidistant sampling w.r.t. v leads to the aliasing frequency

$$f_v^\mathrm{S}(v(u)) = \frac{\mathrm{c}}{\underbrace{|\mathbf{x}'_{0,v}(v(u))| \cdot \Delta_v}_{=\Delta_{\mathbf{x}_0,v}(v(u))} \cdot \gamma(\mathbf{x}_{0,v}(v(u)))} \,. \tag{11}$$

Using (5) together with $\mathbf{x}_{0,u}(u) = \mathbf{x}_{0,v}(v(u))$, $\mathbf{x}'_{0,u}(u) = v'(u)\mathbf{x}'_{0,v}(v(u))$, and $\Delta_u = \Delta_v$ allows to formulate the relation between the aliasing frequencies for the two parametrisations. As $v'(u) > 0$, it reads

$$f_v^\mathrm{S}(v(u)) = v'(u) f_u^\mathrm{S}(u) \,. \tag{12}$$

The resulting optimisation problem is formulated as

$$\underset{v'(u)}{\text{maximise}} \quad \min_u \left[v'(u) f_u^\mathrm{S}(u) \right] \tag{13a}$$

$$\text{subject to} \quad u_\mathrm{max} - u_\mathrm{min} = \int_{u_\mathrm{min}}^{u_\mathrm{max}} v'(\mu) \mathrm{d}\mu \tag{13b}$$

It is shown in the Appendix, that

$$v'_\mathrm{opt}(u) = \frac{(u_\mathrm{max} - u_\mathrm{min})}{\int_{u_\mathrm{min}}^{u_\mathrm{max}} \frac{1}{f_u^\mathrm{S}(\mu)} \mathrm{d}\mu} \frac{1}{f_u^\mathrm{S}(u)} \tag{14}$$

is the solution to the optimisation problem. While the relation between u and v is known, an explicit formula for $\mathbf{x}_{0,v}(v)$ is not available. In order to perform equidistant sampling w.r.t. v, the samples $u^{(n)}$ corresponding to $v^{(n)} = n \cdot \Delta_u + u_\mathrm{min}$ are computed. For this, the equation

$$n \cdot \Delta_u = \int_{u_\mathrm{min}}^{u^{(n)}} v'_\mathrm{opt}(\mu) \mathrm{d}\mu \tag{15}$$

has to be solved. It can be evaluated by combining numerical integration and root finding algorithms. The resulting positions are given by $\mathbf{x}_{0,u}(u^{(n)})$.

5 Simulations

The derived relation between the optimal spacing and the aliasing frequency is discussed with exemplary numerical simulations of the synthesised sound fields. The scenario is depicted in Fig. 3a: A circular SSD with the radius $R = 1.5$ m synthesises a virtual point source at $\mathbf{x}_\mathrm{ps} = [0, 2.5, 0]^\mathrm{T}$ m. The active part of the SSD is illustrated by the black line. A corresponding parametrisation for the active part is given by $\mathbf{x}_{0,u}(u) = R[\sin u, \cos u, 0]^\mathrm{T}$ with $u \in [-\arccos(0.6); \arccos(0.6)]$. The spacing is optimised for eight circular areas of different radii R_l and centres $\mathbf{x}_\mathrm{l}$. Fig. 3b shows the optimised spacings w.r.t. (10) in comparison to equiangular spacing: Here, the virtual sound field was not taken into account. For pos. 2, the optimal spacing is equiangular independent of the radius. A symmetrical pattern with a larger spacing around $u = 0$ can be observed for pos. 1/3. The larger of the two R_l leads to a scheme which is closer to the uniform sampling. This effect is most noticeable for pos. 1. As the scenario for pos. 4 is not symmetric w.r.t. the SSD and the virtual point source, the spacing pattern is also nonsymmetric. Here, the R_l has only a minor effect. The resulting spacings regarding (7) are depicted in Fig. 3c: In general, the additional consideration of the virtual sound field leads to a larger spread of the spacing in comparison to Fig. 3b. Independently of the position, a peak is clearly observable. The u-value corresponding to the peak belongs to the secondary sources, which is exactly in between $\mathbf{x}_\mathrm{l}$ and $\mathbf{x}_\mathrm{ps}$. The magnitude of the peak decreases with increasing R_l (compare solid with dashed) for all four positions. The limiting case (black line), i.e. $R_\mathrm{l} \to \infty$, agrees with this trend.

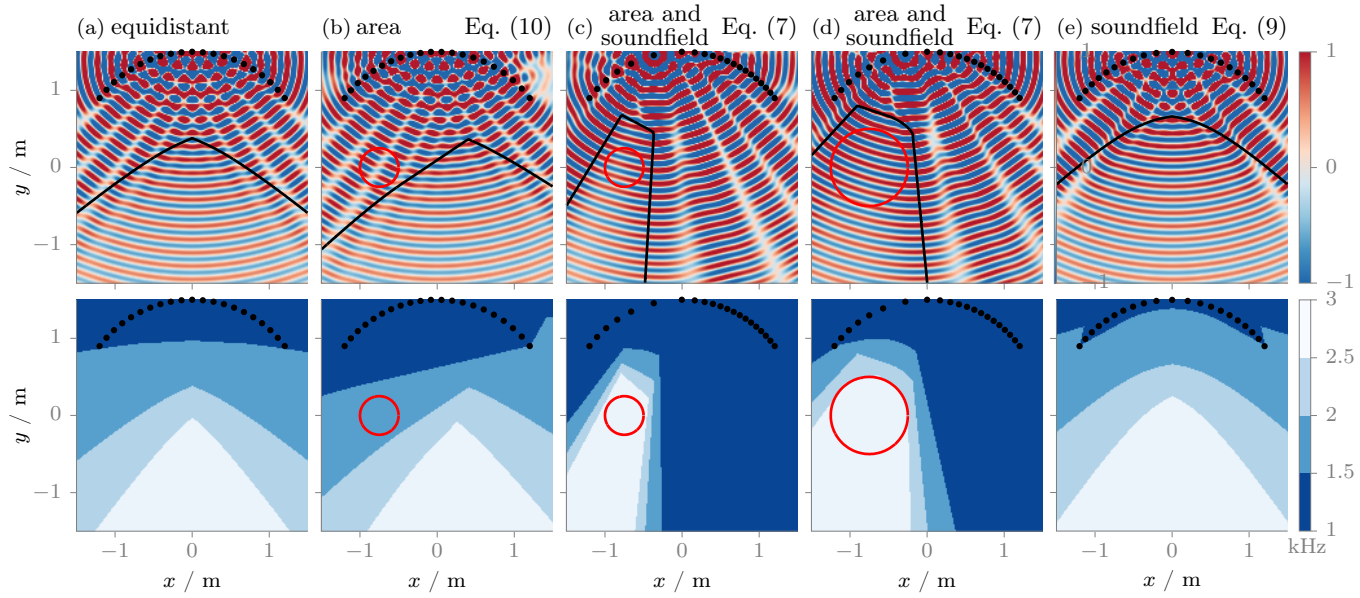

Figure 4: The plots in the top row illustrate a monochromatic ($f = 2$ kHz) virtual point source at $\mathbf{x}_{\mathrm{ps}} = [0, 2.5, 0]^{\mathrm{T}}$ m synthesised by a circular SSD ($N_0 = 21$, black dots) with different spacing patterns. The criteria together with the according function γ, in which regard the patterns are optimised, are given in the title. The area $\mathcal{C}_{\mathrm{l}}$ located at $\mathbf{x}_{\mathrm{l}} = [-0.75, 0, 0]^{\mathrm{T}}$ m with $R_{\mathrm{l}} = 0.25$ m and 0.5 m is drawn red in (b)-(d), respectively. For coordinates above the black line, the predicted aliasing frequency f_v^{S} defined by (5) and (6) is lower than 2 kHz. This frequency is shown in the bottom plots in more detail. A discrete colormap is used for better visibility.

In Fig. 4, the synthesised sound fields and the predicted aliasing frequencies are shown. Compared to the equidistant sampling in Fig. 4a, the optimisation w.r.t. $\mathcal{C}_{\mathrm{l}}$ without considering the virtual sound field does not lead to an improvement of the aliasing properties, see Fig. 4b. This is due to the target function (6) used for optimisation, which defines a worst-case/lower bound for arbitrary sound fields. For a particular virtual sound field, this criterion does not necessarily lead to an increased aliasing frequency. In Fig. 4c and 4d, the additional consideration of the target sound field via (7) increases the aliasing frequency inside $\mathcal{C}_{\mathrm{l}}$. Additional simulations using (7) reveal, that the frequency is about 1.62 ($R_{\mathrm{l}} = 0.25$ m) and 1.48 ($R_{\mathrm{l}} = 0.5$ m) times as high as for the equiangular pattern. The result for an optimisation independent of the listening position is shown in Fig. 4e. Note, that this is equivalent to $R_{\mathrm{l}} \to \infty$. The synthesised sound field and aliasing frequency exhibit a similar structure as for the equiangular case. It agrees with the optimised frequency involving (9) which is 1.16 times as high.

6 Conclusions

This paper investigated on the connection between non-uniform schemes for the discretisation of the SSD and spatial aliasing artefacts in WFS. Based on a generic definition of the spatial aliasing frequency, optimal sampling schemes were found. The joined consideration of the target listening area and the virtual sound field led to the highest improvement. As rule of thumb, a smaller target area allows for larger increase of the aliasing frequency inside it. This was confirmed by numerical simulations of the synthesised sound fields. Future work may incorporate other SFS techniques and directive loudspeakers acting as a spatial lowpass filters.

Appendix

It is assumed that $v'_{\mathrm{opt}}(u)$ given by (14) is *not* the optimal solution: There has to exist a function $w(u)$, such that $v'_{\mathrm{opt}}(u) + w'(u)$ leads to larger minimum (13a) and still fulfils the condition (13b). This leads to

$$0 < w'(u) f_u^{\mathrm{S}}(u) \qquad \forall u \in [u_{\min}, u_{\max}] \tag{16a}$$

$$0 = \int_{u_{\min}}^{u_{\max}} w'(\mu) \mathrm{d}\mu = w(u_{\max}) - w(u_{\min}) \tag{16b}$$

Since the aliasing frequency $f_u^{\mathrm{S}}(u)$ is always positive, the first condition is reformulated to $w'(u) > 0$. Thus, $w(u)$ has to be a strictly increasing function, which violates the second condition. $v'_{\mathrm{opt}}(u)$ has to be the optimal solution.

References

[1] F. Winter, F. Schultz, G. Firtha, and S. Spors. "A Geometric Model for Prediction of Spatial Aliasing in 2.5D Sound Field Synthesis". In: *IEEE/ACM Transactions on Audio, Speech, and Language Processing* (2019).

[2] G. Firtha, P. Fiala, F. Schultz, and S. Spors. "Improved Referencing Schemes for 2.5D Wave Field Synthesis Driving Functions". In: *IEEE/ACM Transactions on Audio, Speech, and Language Processing* 25.5 (2017), pp. 1117–1127.

[3] L. E. Kinsler, A. R. Frey, A. B. Coppens, and J. V. Sanders. *Fundamentals of Acoustics*. 4th Ed. John Wiley & Sons, Inc., 1999.

[4] E. N. G. Verheijen. "Sound Reproduction by Wave Field Synthesis". PhD thesis. Delft University of Technology, 1997.

[5] E. G. Williams. *Fourier Acoustics: Sound Radiation and Nearfield Acoustical Holography*. Academic Press, 1999.